A novel closed-form resistance model for trapezoidal interconnects*

Chen Baojun(陈宝君)[1,2,†], Tang Zhen'an(唐祯安)[1], and Yu Tiejun(余铁军)[3]

(1 School of Electronic Science and Technology, Dalian University of Technology, Dalian 116023, China)
(2 School of Electronics and Information Engineering, Dalian Jiaotong University, Dalian 116028, China)
(3 Department of R&D, Sigrity Inc, USA)

Abstract: A closed-form model for the frequency-dependent per-unit-length resistance of trapezoidal cross-sectional interconnects is presented. The frequency-dependent per-unit-length resistance $R(f)$ of a trapezoidal interconnect line is first obtained by a numerical method. Using the method we quantify the trapezoid edge effect on the resistance of the interconnect and the current density distribution in the cross section. Based on this strict numerical result, a novel closed-form model $R(f)$ for a single trapezoidal interconnect is fitted out using the Levenberg–Marquardt method. This $R(f)$ can be widely used for analyzing on-chip interconnects when the frequency is changing. The model is computationally very efficient with respect to the numerical method, and the results are found to be accurate.

Key words: interconnect; resistance; Levenberg–Marquardt method
DOI: 10.1088/1674-4926/31/8/084011 **EEACC:** 2520

1. Introduction

As circuit complexity increases and MOS devices scale into the deep submicron regime, the interconnect has become a primary bottleneck in integrated circuit design, because the scaling-down technology poses significant challenges to on-chip interconnect design, such as delay, power integrity, and signal integrity[1−3]. Resistance is one of the most important parameters to characterize interconnect behavior. For a digital signal, the frequency spectrum's higher part is more closely related to its rise/drop time t_r (e.g. $1/(3.14t_r)$); this frequency is much higher than the signal frequency itself, and it may be easy reach to tens of gigahertz, therefore, studying the on-chip interconnect $R(f)$ is needed. A simple and accurate interconnect resistance model is the basic requirement in advanced simulation.

Copper (Cu) has been used in deep submicron ULSI technology for many years, but Cu cannot be easily patterned by reactive ion etching (RIE), due to the low volatility of Cu chlorides and Cu fluorides. Therefore Cu interconnects are generally formed using the "dual damascene" process, in which the dielectric is etched before the barrier layer is deposited, by plasma. A sidewall angle is creased and induces a trapezoidal shape of the copper line. The trapezoidal copper line causes a decreasing cross section that leads to a resistance increase compared to the rectangular line. The increased resistance caused by the trapezoidal edge will provide a consistent decrease on the transmission properties of the line. Therefore the importance of modeling the trapezoidal edge is highlighted[4−7]. Scogna[5] quantifies the trapezoidal shape effect on the electrical performance to stripline. Travaly[6,7] points out that the resistance is linear to the reciprocal of the cross section of the line and analyzes how the profile of the line influences the resistance heavily. But none of them clearly calculate the resistance of the trapezoidal copper line or give the closed model.

In this paper, we first develop a numerical method to calculate the resistance of the trapezoidal copper line and try to figure out the final $R(f)$ changes based on which parameters change and in which way. We also give the current distribution in the cross section of the conductor. Then a closed-form model is fitted out using the Levenberg–Marquardt method based on the numerical results. The final comparison proves that the model has obvious advantages in the accuracy and efficiency in simulation and it can be used in local, intermediate and global interconnects.

2. Numerical method for resistance extraction considering the skin effect

To capture the interconnect skin effect accurately, we first develop a numerical method to calculate frequency-dependent per-unit-length resistance of trapezoidal cross sectional interconnect.

Figure 1 is the cross section of the line used in this paper.

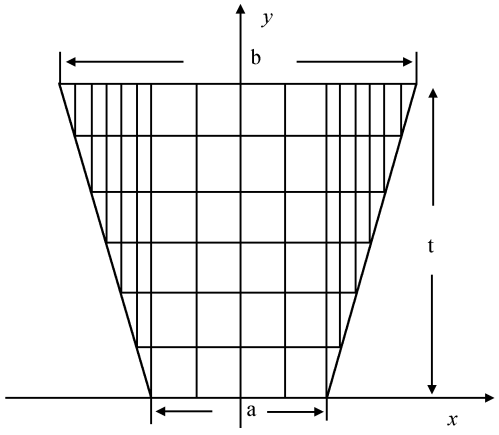

Fig. 1. Trapezoidal line and its discretization of mesh.

* Project supported by the National Natural Science Foundation of China (No. 90607003).
† Corresponding author. Email: beec98@163.com
Received 27 January 2010, revised manuscript received 10 March 2010

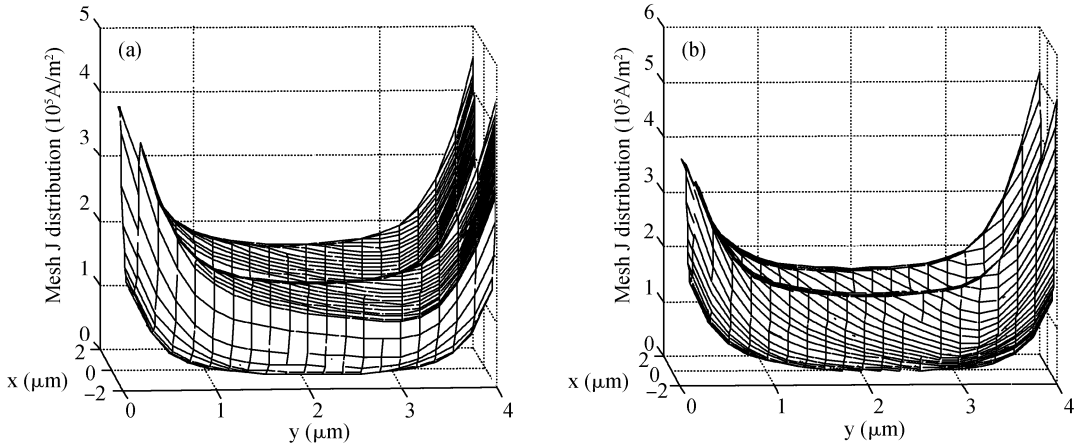

Fig. 2. 3D topographic plot of current density distribution over a cross section of the line. The dimensions are: $b = 4$ μm, $t = 4$ μm. (a) $a = 3.5$ μm. (b) $a = 2$ μm.

a is the width of the lower edge, b is the width of the upper edge and t is the height of the line. The trapezoidal line is discretized into a collection of parallel thin filaments through which current is assumed to flow uniformly. The filaments are hybrid, including triangle and rectangle.

For each filament, it has a resistance r and inductance l; between the different filaments there is inductance coupling, so the system equation can be generated as:

$$V = zI, \tag{1}$$

where V is the per-unit-length voltage drop on the line. V and I are a vector with a number of N ($N = N_\mathrm{P} + N_\mathrm{g}$), and N_P and N_g are the trapezoidal line discretization number and its image line's discretization number. The z matrix can be expressed as:

$$\left[z_{ij}\right]_{N\times N} = \left[r_{ij}\right]_{N\times N} + \mathrm{j}\omega\left[l_{ij}\right]_{N\times N}, \tag{2}$$

where

$$r_{ij} = \begin{cases} \dfrac{1}{\sigma A_i}, & i = j, \\ 0, & i \neq j, \end{cases} \tag{3}$$

and

$$l_{ij} = -\frac{\mu_0}{4\pi A_i A_j}\int_{S_i}\int_{S_j}\ln\left[\left(x-x'\right)^2 + \left(y-y'\right)^2\right]\mathrm{d}S_i\,\mathrm{d}S_j, \tag{4}$$

where A_i is the cross sectional area of the filament.

The 2D boundary elemental method (BEM) is used to calculate Eq. (4) and the formula is

$$l_{ij} = \begin{cases} f(x,y/x',y')|_{-0.5a}^{0.5a}|_{-0.5t}^{0.5t}|_{-0.5b}^{0.5b}|_{-0.5t}^{0.5t} + \dfrac{25}{6}\times 10^{-7} \\ \quad -\dfrac{\mu_0}{4\pi A_i A_j}\displaystyle\sum_{m}^{N_1}\sum_{n}^{N_2}\sum_{m'}^{N_3}\sum_{n'}^{N_4} w_m w_n w_{m'} w_{n'}, \ i = j, & \text{(5a)} \\ \ln[(x_{im} - x_{jm'})^2 + (y_{in} - y_{jn'})^2], \ i \neq j. & \text{(5b)} \end{cases}$$

In Eq. (5b), N_1, N_2, N_3, N_4 are Gaussian quadrate orders in the x and y directions, and w_m, w_n, w'_m, w'_n are the corresponding weights. To ensure accuracy we use Eq. (5a) to calculate the self inductance[8]. The definitions are $f(x)|_x^y = f(y) - f(x)$ and $f\,(X,Y) = \frac{\mu_0}{96\pi A_i^2}\left\{\left[X^4 + Y^4 - 6X^2Y^2\right]\ln(X^2 + Y^2) - 8XY\left[X^2\tan^{-1}(Y/X) + Y^2\tan^{-1}(X/Y)\right]\right\}$, $X = x - x'$, $Y = y - y'$.

All the filaments in the trapezoidal line have the same cross voltage and voltage drop along the line length. The filaments in the trapezoidal line have their own current, and the summation of all the filaments' current is the final trapezoidal line's current. Therefore, by solving Eq. (1) one can obtain the current distribution as:

$$I = z^{-1}V = yV. \tag{6}$$

Based on the above assumptions, the $N \times N$ filament l and r matrices can be size reduced to 2×2 matrices by the following approach:

$$\left[y_{ij}\right]_{N\times N} = \left[z_{ij}\right]^{-1}, \tag{7}$$

$$\left[Y_{ij}\right]_{2\times 2} = \begin{bmatrix} Y_{\mathrm{pp}} & Y_{\mathrm{pg}} \\ Y_{\mathrm{gp}} & Y_{\mathrm{gg}} \end{bmatrix}, \tag{8}$$

where

$$Y_{\mathrm{pp}} = \sum_{i=1}^{N_\mathrm{P}}\sum_{j=1}^{N_\mathrm{p}} y_{ij}, \quad Y_{\mathrm{pg}} = \sum_{i=1}^{N_\mathrm{P}}\sum_{j=N_\mathrm{p}+1}^{N} y_{ij},$$

$$Y_{\mathrm{gp}} = \sum_{i=N_\mathrm{p}+1}^{N}\sum_{j=1}^{N_\mathrm{p}} y_{ij}, \quad Y_{\mathrm{gg}} = \sum_{i=N_\mathrm{p}+1}^{N}\sum_{j=N_\mathrm{p}+1}^{N} y_{ij}. \tag{9}$$

Then for the inverse of the 2×2 Y matrix one obtains the 2×2 Z matrix:

$$\left[Z_{ij}\right]_{2\times 2} = R + \mathrm{j}\omega L = \begin{bmatrix} r_{\mathrm{pp}} + \mathrm{j}\omega l_{\mathrm{pp}} & r_{\mathrm{pg}} + \mathrm{j}\omega l_{\mathrm{pg}} \\ r_{\mathrm{gp}} + \mathrm{j}\omega l_{\mathrm{gp}} & r_{\mathrm{gg}} + \mathrm{j}\omega l_{\mathrm{gg}} \end{bmatrix} = \begin{bmatrix} Y_{\mathrm{pp}} & Y_{\mathrm{pg}} \\ Y_{\mathrm{gp}} & Y_{\mathrm{gg}} \end{bmatrix} \tag{10}$$

Finally, real(Z_{11}) is the trapezoidal line's frequency-dependent per-unit-length resistance. This technique is used in some software such as FastHenry to calculate a rectangular line's frequency-dependent per-unit-length resistance[9] and the results are accurate.

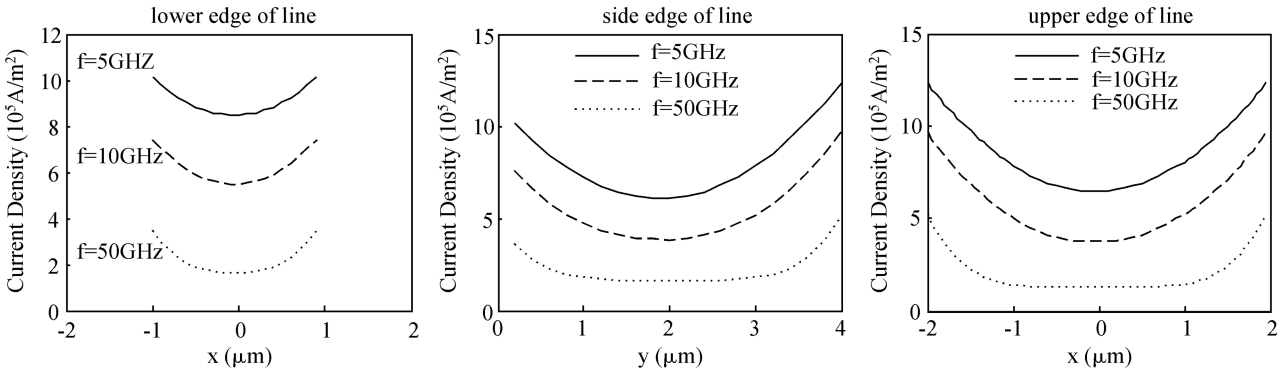

Fig. 3. Distribution of current density on the boundary of a single line at different frequencies. The dimensions are: $b = 4$ μm, $a = 2$ μm, $t = 4$ μm.

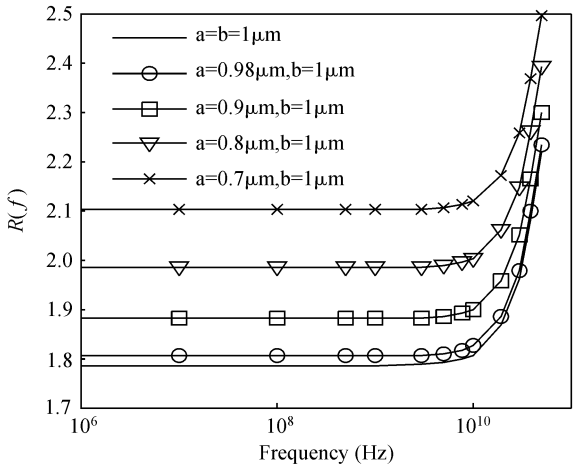

Fig. 4. Frequency-dependent per-unit-length resistance of a trapezoidal line, $t = 1$ μm.

Figure 2 shows the 3D topography of a normalized axial current density distribution over a cross-section of the conductor. Clearly, the current distribution is symmetric with respect to $x = 0$. Due to the trapezoidal cross section the upper two angles are sharp ones and explicit edge behavior becomes sharper. So the differential value of current density between the upper edge and lower edge becomes larger as the differential width value increases.

Figure 3 presents the current density on the boundary line. It shows that the edge behavior becomes sharper as the frequency f assumes larger values. So it is found numerically that the cross-section current density distribution of a single conductor depends on the thickness, the upper width, the lower width and the frequency.

Figure 4 presents the frequency-dependent per-unit-length resistance for a single trapezoidal line. From the figure we can see that when the width of the lower edge decreases from the upper width the DC resistance assumes a bigger value compared with the standard rectangular cross-section. For different lower widths, all the $R(f)$ are convergent to the $R_{\rm dc}$ at low frequency. As the frequency is increased, the fine line first shows skin effects while the narrower line shows the skin effect later.

3. Closed-form model

In the model that we propose here, the frequency-dependent resistance is represented as:

$$\begin{cases} R_l(f) = R_{\rm dc} + m(f/f_0) + n(f/f_0)^2, & f < f_0, \quad (11a) \\ R_h(f) = R_{\rm dc}{\rm e}^{k+(0.5-q)\ln(f/f_0)}, & f \geqslant f_0, \quad (11b) \end{cases}$$

where $R_{\rm dc}$ is the direct resistance, f_0 is the break frequency $f_0 = \frac{4}{\pi\mu_0\sigma}\left(\frac{b+t}{bt}\right)^2$, and k, q, m, n are constants to be described.

Equation (11a) is used to compute the resistance in the range of low frequency and it ensures $R(f)$ is equal to $R_{\rm dc}$ at zero frequency. Equation (11b) corresponds to the high frequency and the resistance varies as $\sqrt{f}$. To maintain the continuity of the two formulae of $R(f)$ at f_0 we use two equations to get the parameters m, n in Eq. (11a).

$$[R_l(f) = R_h(f)]\big|_{f=f_0}, \quad (12)$$

$$[{\rm d}R_l(f)/{\rm d}f = {\rm d}R_h(f)/{\rm d}f]\big|_{f=f_0}, \quad (13)$$

where Equation (11) shows the continuity of the $R(f)$ and Equation (13) shows the smoothness at the turning points.

Then it can be found that

$$m = R_{\rm dc}{\rm e}^k(1.5+q) - 2R_{\rm dc}, \quad (14)$$

$$n = R_{\rm dc} - R_{\rm dc}{\rm e}^k(0.5+q). \quad (15)$$

The parameters k, q are determined by the size of the dimension of the line and their values can be calculated by the Levenberg–Marquardt method.

The Levenberg–Marquardt method[10] is an iterative technique that locates the minimum of a multivariate function that is expressed as the sum of the squares of non-linear real-valued functions. It has become a standard technique for non-linear least-squares problems.

In the Levenberg–Marquardt method, the performance index $f(\boldsymbol{w})$ to be minimized is defined as the sum of squared errors, namely

$$F(\boldsymbol{w}) = \boldsymbol{e}^T\boldsymbol{e}, \quad (16)$$

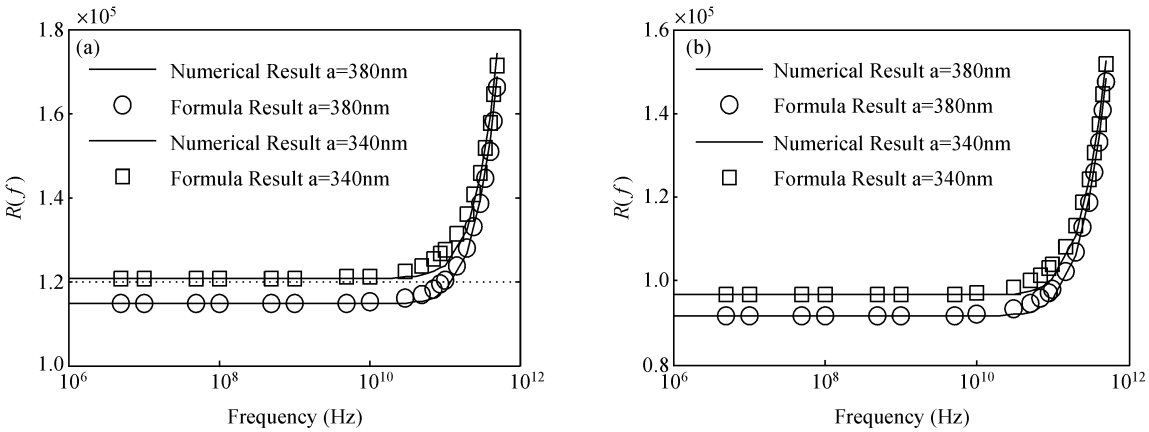

Fig. 5. Comparison $R(f)$ between our Eq. (3) and the numerical method. Line size is: (a) b = 400 nm, t = 400 nm. (b) b = 400 nm, t = 500 nm.

where $\boldsymbol{w} = [k, q]^T$ consists of the two parameters, and $\boldsymbol{e}$ is the error vector.

The increment of weights $\Delta \boldsymbol{w}$ can be obtained as follows:

$$\Delta \boldsymbol{w} = \left[\boldsymbol{J}^T \boldsymbol{J} + \lambda \boldsymbol{I}\right]^{-1} \boldsymbol{J}^T \boldsymbol{e}, \tag{17}$$

where $\boldsymbol{J}$ is the Jacobian matrix, and λ is the damping term which is to be updated using the decay rate β depending on the outcome. In particular, λ is multiplied by the decay rate β ($0 < \beta < 1$) whenever $F(\boldsymbol{w})$ decreases, while λ is divided by β whenever $F(\boldsymbol{w})$ increases in a new step.

The standard Levenberg–Marquardt method can be illustrated in the following steps:

(1) Initialize the two parameters k,q and λ ($\lambda = 0.01$ is appropriate);

(2) Compute the sum of squared errors $F(\boldsymbol{w}_i)$;

(3) Compute the Jacobian matrix $\boldsymbol{J}_i$;

(4) Solve Eq. (17) to obtain the increment $\Delta \boldsymbol{w}_i$;

(2) Recompute the sum of squared errors $F(\boldsymbol{w}_i')$ using $\boldsymbol{w}_i + \Delta \boldsymbol{w}_i$ as the trial $\boldsymbol{w}_i'$. If $F(\boldsymbol{w}_i')$ is less than$F(\boldsymbol{w}_i')$, the next increment $\boldsymbol{w}_{i+1} = \boldsymbol{w}_i + \Delta \boldsymbol{w}_i$ and the damping term $\lambda_{i+1} = \lambda_i \beta$ ($\beta = 0.1$). Then go back to Step 2. If $F(\boldsymbol{w}_i')$ is bigger than $F(\boldsymbol{w}_i)$ the damping term $\lambda_{i+1} = \lambda_i / \beta$ and the iteration is stopped.

Using the Levenberg–Marquardt method we obtain large numbers of values of k, q. By analysis they can be expressed by

$$k = k_c + k_s \frac{b-a}{t}, \tag{18}$$

$$q = q_c + q_s \frac{t}{b-a}, \tag{19}$$

where:

$$q_c = 0.051 - 61417.7t + 10^{11} t^2, \tag{20}$$

$$q_s = 1.3195 \times 10^{-4} - 2.417 \times 10^{-5} \left(\frac{t}{b}\right)^2 - 2 \times 10^9 b^2 + 4 \times 10^8 t^2, \tag{21}$$

$$k_c = 0.354 + 107751.1t - 4 \times 10^{11} b^2, \tag{22}$$

$$k_s = -0.14 + 0.37 \frac{t}{b} + 234035.5t. \tag{23}$$

The coefficients in Eqs. (20)–(23) are also obtained by the Levenberg–Marquardt method.

So Equation (11a) combined with Eq. (11b) constitutes our final closed-form model for a single trapezoidal line's p.u.l. (per-unit-length) $R(f)$ and the parameters in Eq. (3) can be calculated by Eqs. (14), (15) and (18)–(23).

4. Results

Model (3) is an explicit expression that contains the frequency and the line size as variables. To validate the model, we compare it with the numerical results.

Figure 5 shows a comparison between the different resistance values for a single line. The numerical results are regarded as the standard true results. From the picture, one can see that our proposed model results always agree well with the numerical results in the whole frequency range and with different dimension sizes. The maximal relative error is less than 4%. The model can calculate the resistance of a trapezoidal copper interconnect in nanotechnology; it is valid in the range of 100 nm $\leqslant b \leqslant$ 600 nm, $1 \leqslant$ AR $\leqslant 2$ (AR $= b/t$), $0 < (b-a)/t \leqslant 0.2$.

The numerical method is accurate if the trapezoidal line is divided into enough small filaments. However, as the number of filaments increases, the computation complexity is also increased quickly as N size matrix z inversion is required, so it will take more time to compute the resistance. For example, a trapezoidal line (with dimensions of a = 340 nm, b = 400 nm, t = 400 nm) is divided into 210 filaments and it takes 1406 ms to compute the resistance while model (3) takes only 0.1 ms. So the obvious advantage of model (3) is its high efficiency.

5. Conclusion

In this paper, we use a numerical method to calculate the frequency-dependent resistance of a trapezoidal cross-sectional conductor. The effect of the trapezoidal edge on the resistance of the standard trapezoidal conductor is analyzed. A closed-form model of the frequency-dependent resistance of the trapezoidal line is presented in Eq. (3). It is fitted out in

the Levenberg–Marquardt method based on accurate numerical results. Compared to the numerical method, the formula has obvious advantages in its efficiency varying ranges. The proposed model can be used widely in CAD simulation of IC levels for power or signal integrity.

References

[1] Chen G, Chen H, Haurylau M. Electrical and optical on-chip interconnects in scaled microprocessors. Circuits and Systems, 2005, 3: 2514

[2] Gambino J, Chen F, He J. Copper interconnect technology for the 32 nm node and beyond. IEEE Custom Integrated Circuits Conference, 2009: 141

[3] Wang X, Liu D, Yu W, et al. Improved boundary element method for fast 3-D interconnect resistance extraction. IEICE Trans Electron, 2005, 2: 232

[4] Vilmay M, Roy D, Monget C. Copper line topology impact on the reliability of low-k SIOCH for the 45nm technology node and beyond. Integrated Reliability Workshop Final Report, 2008: 16

[5] Scogna A C, Schauer M. Stripline simulation model with tapered cross section and conductor surface profile. Electromagnetic Compatibility, 2007: 1

[6] Travaly Y, Mandeep B, Carbonell L. On a more accurate assessment of scaled copper/low-*k* interconnects performance. Semicond Manuf, 2007, 20: 333

[7] Kapur P, McVittie J P, Saraswat K C. Technology and reliability constrained future copper interconnects: I. resistance modeling. IEEE Trans Electron Devices, 2002, 49: 590

[8] Weeks W T, Wu L L, McAllister M F, et al. Resistive and inductive skin effect in rectangular conductors. IBM Journal of Research and Development, 1979, 6: 652

[9] Wei Hongchuan, Yu Wenjian, Yang Liu, et al. Fast inductance and resistance extraction of 3-D VLSI interconnects based on the method of K element. Acta Electronica Sinica, 2005, 33(8): 1635

[10] Madsen K, Nielsen H B, Tingleff O. Methods for non-linear least squares problems. Informatics and Mathematical Modeling Technical University of Denmark, 2004: 24